



## Experimental and numerical study of reverberation time of an enclosed room

Sumit Mehta<sup>1</sup> and Ashish Purohit<sup>2\*</sup>

<sup>1,2</sup>Mechanical Engineering Department, Thapar Institute of Engineering and Technology  
Patiala-147004, India

\*Corresponding author: ashish.purohit@thapar.edu

### **Abstract**

The problem of room acoustics has been studying from several decades; however it has always been complicated to understand sound propagation in an enclosed space and its control for better hearing. In the present work, numerical and experimental investigations of sound propagation within a three-dimensional closed space are carried out and acoustic characteristic of an enclosed space is estimated by measuring reverberation time. For the numerical study, linear wave equation is discretized by finite difference technique and to realize reflection/absorption effect from the wall boundary, different boundary conditions are employed. The developed numerical methodology is validated for benchmark studies and reverberation time of a room is computed. Experiments are conducted to measure reverberation time of a classroom by pricking a balloon and by a harmonic sound source. The numerical results obtained show reasonable matching with experimental results and obtained reverberation time indicates that the classroom may be treated acoustically to improve reverberation time required for effective lecturing.

**Key words:** Reverberation time, wave equation, finite difference schemes, reflecting surface, absorbing boundary condition, sound source

### **1. Introduction**

Analysis of sound propagation in an enclosed space is challenging, however important for designing an architectural acoustics of the space. Acoustic wave experiences absorption and reflection from the wall boundaries which affects the reverberation time (RT) of enclosed space and so the hearing quality at the receiver end. Although, from the acoustical point of view, designed value of RT is different for different spaces like classroom, living room and auditorium. It may be noted that the acoustics of a room is more an experimental phenomenon and it is very difficult to understand the wave behavior theoretically [1]. The problem of room acoustics has been investigated from several decades and has been a challenging field for the researchers. Particularly, numerical modeling of acoustic boundary conditions for a three dimensional space is very challenging. In the present investigation, a problem of estimation of reverberation time of a three dimensional classroom including different wall boundary condition is numerically solved and experimentally validated.

Sabine [2] has conducted a series of experiments and proposed a basic formula to calculate reverberation time of a room. Later on, he has modified his formulation to optimize RT by studying

architectural acoustic of a room. Eyring [3] has been modified the Sabine's formulation by incorporating higher value of absorption coefficient. Kuttruff [1] generalized the reverberation time formula by taking the average value of absorption coefficient considering multiple reflections at the wall. As the reflection and absorption of sound wave depend on the material of wall boundary, a number of experimental studies have been carried out in the past to identify the acoustical property of different material e.g. fibrous material [4], wood based materials [5-6] etc. Recently, in the last two decades, after the advancement of the computational infrastructure, study of architectural acoustics through the numerical simulation has been practiced. Botteldooren[7] has numerically investigated the reverberation time of an auditorium. He discretized linear wave equation using finite difference time domain (FDTD) scheme and studied the low and mid frequency sound (63 Hz and 125 Hz) propagation in the auditorium. He concluded that the attenuation of low frequency sound in the room is difficult than the high frequency sound. Kowalczyk and Walstijn[8] have extended the Botteldooren's work, however, they extensively worked on the acoustical boundary condition. They have introduced locally reacting surface type boundary condition to simulate different level of absorption and reflection of sound from the wall boundary. They proposed a formulation for both frequency dependent and independent wall boundaries [7-8]. It is observed that in most of the previous investigations, the focus of the study is either on the development of an advanced numerical method [9-11] or on the estimation of reverberation time through experiments. A comprehensive investigation of room acoustics including both experimental and numerical work is rare.

In this paper, reverberation time of a classroom is obtained by both experimental and numerical ways. For numerical study, linear wave equation is discretized spatially and temporally with finite difference method (FDM) and various boundary conditions are implemented to study different level of absorption and reflection of sound from wall surfaces. Numerical formulation for wave propagation is developed for one, two and three dimensional domains and validated for sound propagation from different sound source as point source, line source and pulsating cylindrical source. Experiments are conducted in a classroom using a harmonic sound source as well as by an impulse sound source (balloon pricking).

## 2. Numerical methodology and problem definition

Wave propagation is governed by wave equation derived from the hydrodynamics and adiabatic relationship between pressure and density. There are different numerical techniques as finite difference method, finite element technique, etc., are practiced to simulate acoustic propagation. Unlike finite element methods (FEM), finite difference approach is straight forward approach and more suitable for virtual spaces with moving sound source and receiver [10]. Among the different available finite difference schemes as Lax-Wendroff, Lax-Friedrich, Forward Time Center Space (FTCS), Leapfrog scheme, etc., last scheme shows relatively lower diffusion of the sound and low numerical error [7-8, 10]. Therefore, in the present study, Leapfrog scheme is considered to solve wave propagation.

### 2.1 Discretization of wave equation

The governing wave equation is a second order partial differential hyperbolic equation in which second order forward difference terms are used for both time and spatial derivatives.

$$\frac{\partial^2 p}{\partial t^2} = c^2 \frac{\partial^2 p}{\partial x^2} \quad (1)$$

$$\frac{p_x^{ts+1} - 2p_x^{ts} + p_x^{ts-1}}{\Delta t^2} = c^2 \frac{p_{x+1}^{ts} - 2p_x^{ts} + p_{x-1}^{ts}}{\Delta x^2} \quad (2)$$

Equation (1) is one dimensional wave equation that indicates how the curvature of wave-front is balanced by the rate of change of pressure. Eq. (2) shows discretization of (1) in both spatial and temporal dimensions, where,  $\Delta t$  and  $\Delta x$  are temporal and spatial step size respectively. The explicit value of pressure ( $p$ ) at the next time step  $ts + 1$  is calculated as:

$$p_x^{ts+1} = \lambda^2 (p_{x+1}^{ts} + p_{x-1}^{ts}) + 2p_x^{ts} (1 - \lambda^2) - p_x^{ts-1} \quad (3)$$

Similarly, for the two and three dimensional fields, acoustic pressure at a point in space can be calculated as:

$$p_{x,y}^{ts+1} = \lambda^2 (p_{x+1,y}^{ts} + p_{x-1,y}^{ts} + p_{x,y+1}^{ts} + p_{x,y-1}^{ts}) + 2p_{x,y}^{ts} (1 - 2\lambda^2) - p_{x,y}^{ts-1} \quad (4)$$

$$p_{x,y,z}^{ts+1} = \lambda^2 (p_{x+1,y,z}^{ts} + p_{x-1,y,z}^{ts} + p_{x,y+1,z}^{ts} + p_{x,y-1,z}^{ts} + p_{x,y,z+1}^{ts} + p_{x,y,z-1}^{ts}) + 2p_{x,y,z}^{ts} (1 - 3\lambda^2) - p_{x,y,z}^{ts-1} \quad (5)$$

In Equations (4-5), term  $\lambda = c \frac{\Delta t}{\Delta x}$  is a constant that is important to decide the stability of explicit numerical solution of wave propagation. For the stable solution, the value of  $\lambda$  is considered less than 1,  $\frac{1}{\sqrt{2}}$  and  $\frac{1}{\sqrt{3}}$  for one, two and three dimensional numerical simulations respectively [12].

## 2.2 Acoustic boundary condition

In the case of acoustic propagation within enclosed space, interaction of sound from the boundary is a complex phenomenon and must be defined correctly to simulate accurate results. Impedance due to boundary resists the wave motion, which results in reflection, absorption or transmission of wave. At the boundary, solution of Equation (1-3) need pressure value at all the points lie beyond the boundary, e.g. in case of one dimension (3) solution, either  $p_{x+1}^{ts}$  or  $p_{x-1}^{ts}$  will be required to solve right and left boundaries respectively. These points beyond the computational domain are called ghost points and suitable governing equation is required to estimate pressure values at the ghost points. One of the approaches is to use advection equation to solve ghost point at the boundaries.

$$\frac{\partial p}{\partial t} \pm c \frac{\partial p}{\partial x} = 0 \quad (6)$$

Equation (6) is a set of advection equations, which give solution of propagating wave in both forward and backward direction individually. In (6), term  $c$  is speed of travelling disturbance and  $p$  indicates disturbance amplitude. In the case of one dimensional forward travelling wave, which is interacting with the right side boundary, the advection term can be expressed as

$$\frac{\partial p}{\partial t} = -\zeta c \frac{\partial p}{\partial x} \quad (7)$$

$$\frac{p_x^{ts+1} - p_x^{ts-1}}{2\Delta t} + c\zeta \frac{p_{x+1}^{ts} - p_{x-1}^{ts}}{2\Delta x} = 0 \quad (8)$$

Equation (8) shows the FDTD formulation of (7), where  $\zeta$  is specific impedance [1], defined as the ratio of wall impedance  $z = \frac{p}{u_x}$  and characteristic impedance ( $\rho c$ ). The specific impedance is also defined as  $\zeta = \frac{R+1}{R-1}$ , where  $R$  is reflection coefficient of wall material, which can be experimentally evaluated with standard short tube impedance method [13]. Pressure value at the right side boundary ghost point ( $p_{x+1}^{ts}$ ) is calculated using central difference approach as

$$\frac{\partial p}{\partial x} = \frac{p_{x+1}^{ts} - p_{x-1}^{ts}}{2\Delta x} \quad (9)$$

and by (7-9), explicit value of acoustic pressure at time  $ts+1$  is obtained by:

$$p_x^{ts+1} = \frac{2\lambda^2 p_{x-1}^{ts} + 2p_x^{ts} (1 - \lambda^2) + p_x^{ts-1} (\lambda / \zeta - 1)}{\lambda / \zeta + 1} \quad (10)$$

Similarly for the left boundary, equation (6) with negative sign will be considered. In case of wave propagation in two and three dimensional spaces, two and three dimensional advection equations are implemented.

$$p_{x,y}^{ts+1} = \frac{\lambda^2(2p_{x-1,y}^{ts} + p_{x,y+1}^{ts} + p_{x,y-1}^{ts}) + 2p_{x,y}^{ts}(1 - 2\lambda^2) - p_{x,y}^{ts-1}(\frac{\lambda}{\zeta_x} - 1)}{(\frac{\lambda}{\zeta_x} + 1)} \quad (11)$$

$$p_{x,y,z}^{ts+1} = \frac{\lambda^2(2p_{x-1,y,z}^{ts} + p_{x,y+1,z}^{ts} + p_{x,y-1,z}^{ts} + p_{x,y,z+1}^{ts} + p_{x,y,z-1}^{ts}) + 2p_{x,y,z}^{ts}(1 - 3\lambda^2) - p_{x,y,z}^{ts-1}(\frac{\lambda}{\zeta_x} - 1)}{(\frac{\lambda}{\zeta_x} + 1)} \quad (12)$$

Eq. (11) and Eq. (12) represent finite different formulation of wave at the boundary for two and three-dimensional cases. The given formulation is illustrating interaction of wave at right boundary (along positive x direction). In above equations,  $\zeta_x$  is the specific impedance for right boundary in x direction. Similarly, for other boundaries, different formulation with different  $\zeta$  are employed. In addition to boundary point, modeling of corner points is a critical aspect. Figure 1 shows corner point at the right boundary of a two dimensional computational domain. The corner point shares the impedance of all adjacent boundaries and, thus, needs care in the modeling.

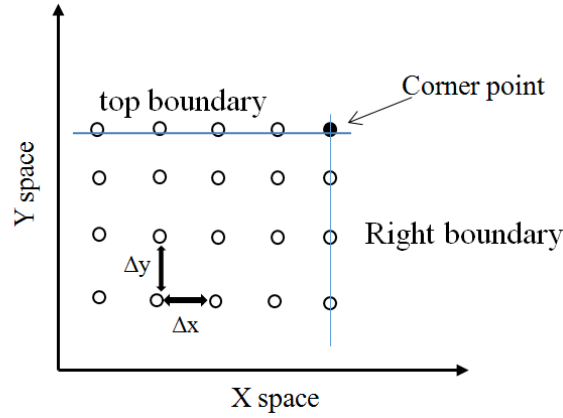


Figure 1: Acoustic computational domain showing boundaries and corner point.

$$p_{x,y}^{ts+1} = \frac{\lambda^2(2p_{x-1,y}^{ts} + 2p_{x,y-1}^{ts}) + 2p_{x,y}^{ts}(1 - 2\lambda^2) - p_{x,y}^{ts-1}(\frac{\lambda}{\zeta_x} + \frac{\lambda}{\zeta_y} - 1)}{(\frac{\lambda}{\zeta_x} + \frac{\lambda}{\zeta_y} + 1)} \quad (13)$$

$$p_{x,y,z}^{ts+1} = \frac{\lambda^2(2p_{x-1,y,z}^{ts} + p_{x,y+1,z}^{ts} + p_{x,y-1,z}^{ts} + p_{x,y,z+1}^{ts} + p_{x,y,z-1}^{ts}) + 2p_{x,y,z}^{ts}(1 - 3\lambda^2) - p_{x,y,z}^{ts-1}(\frac{\lambda}{\zeta_x} + \frac{\lambda}{\zeta_y} + \frac{\lambda}{\zeta_z} - 1)}{(\frac{\lambda}{\zeta_x} + \frac{\lambda}{\zeta_y} + \frac{\lambda}{\zeta_z} + 1)} \quad (14)$$

Equation (13) and (14) show modeling of acoustic pressure at the right corner point for two and three dimensions respectively.  $\zeta_x$ ,  $\zeta_y$  and  $\zeta_z$  are the impedances in x, y and z direction respectively. In the case of wave propagation in two and three dimensional spaces, the interaction of wave front with the wall surface is not same as in the case of one dimensional planer wave, in which the angle of incidence is always orthogonal to the wall surface. However, In the case of two-dimensional wave propagation, there may be an angle between wave front and normal of the wall surface, which influences the reflection and

absorption of the wave. The angularity can be modeled by including the incidence angle, in the expression of specific impedance. Although, in the previous investigations, it is noted that consideration of effect of incidence angle has minor variation in the reverberation time [8] and hence, for the simplification, it has not been considered in the present numerical investigations. For the solution, a MATLAB code is developed in house and validated for various benchmark problems.

## 2.3 Validation of Numerical Methodology

### One-dimensional propagation of sound wave:

In this section, a case study of one dimensional plane sound wave propagation and its reflection/absorption from the boundary is discussed. For this purpose, a harmonic point source of strength  $p = 5 \sin(\omega t)$  of frequency 100 Hz and amplitude of 5 Pa is considered. The computational space is discretized with a spatial step size  $\Delta x = 0.2\text{m}$ . Time step is calculated by using *CFL* criterion, which yields  $\Delta t = 0.00041\text{seconds}$  for velocity of sound 340 m/s. For the boundary surface, four different reflection coefficients 0.3, 0.5, 0.7 and 1 are considered. The pressure is measured at a fixed distance from the boundary (point P) and RMS value of pressure is compared for both incident and reflected waves. Schematic propagation of wave motion and its reflection from the wall is shown in Figure 2. It is observed that the reflected wave is superimposed on the incident wave and the resultant wave has increased amplitude. Figure 3 shows the time history of the pressure for various reflections coefficient measured at a location (point P) near to the right boundary.

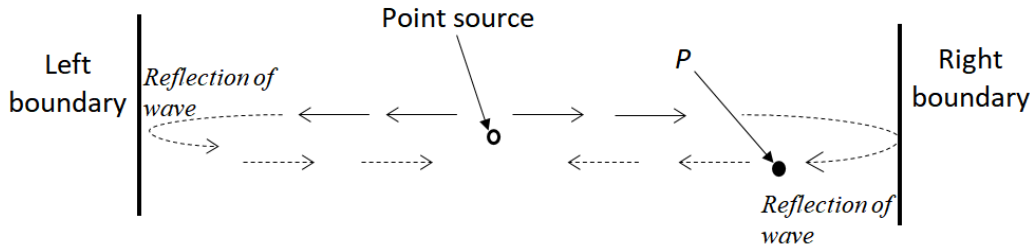


Figure .2 One dimensional wave propagation and its reflection from boundary.

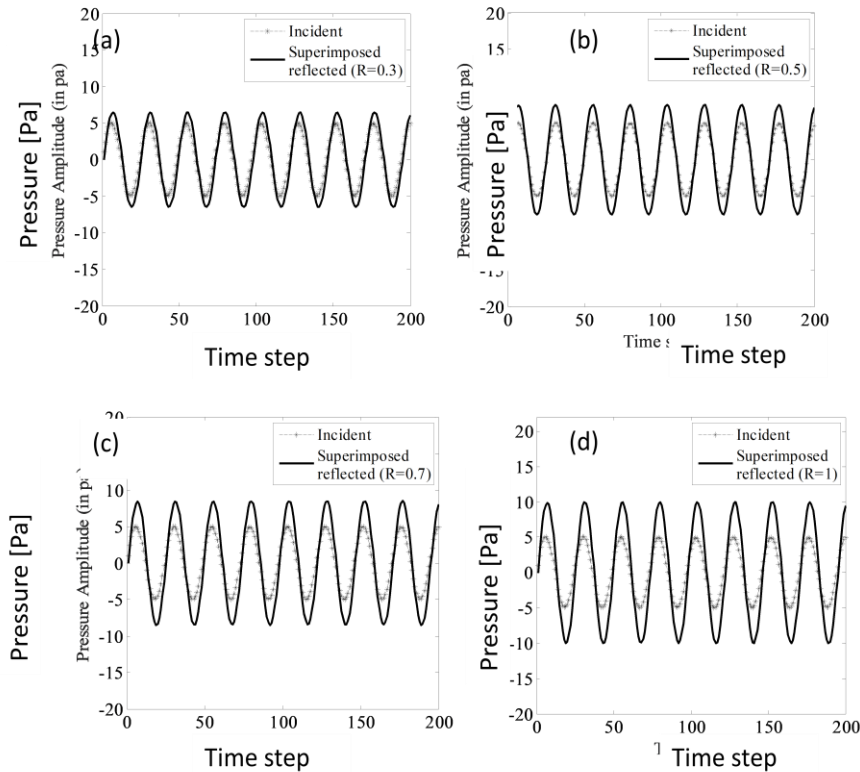


Figure 3. Time history of incident and reflected wave (superimposed) at point P for reflection coefficient, a) 0.3, b) 0.5, c) 0.7 & d) 1

In Figure 3, the pressure of incident wave is shown by dotted line and reflected wave (superimposed wave) is presented by solid line. Table 1 shows the RMS pressure amplitude of the incident wave, superimposed wave and reflected wave. The amplitude of reflected wave is calculated by subtracting column 4 and 3 of Table 1, which reflects the amount of reflection coefficient provided to the wall, e.g. for a reflection coefficient 0.3 (Table 1 column 2), the amplitude of the reflected wave is close to 30 percent (Table 1 column 6) of the incident wave. It is noted that the reflected wave has a minor phase shift, which may be due to the discretization error in the FDTD scheme. However, the RMS value is independent of the phase shift; therefore, comparison of RMS pressure suffices the effectiveness of the reflection coefficient in the formulation.

Table 1. Comparison of RMS values corresponds to reflection coefficient

S. No	Reflection Coefficient (R)	RMS Value of incident wave	RMS Value of superimposed-reflected wave	RMS value of reflected wave	Percentage change in RMS value
1	0.3	3.5276	4.5674	1.0392	29.48
2	0.5	3.5276	5.2743	1.7467	49.52
3	0.7	3.5276	5.9825	2.4549	69.59
4	1	3.5276	7.0473	3.5197	99.78

#### Two-dimensional sound radiation from pulsating cylinder:

In this section, sound propagation in two dimensional space is checked. A pulsating cylindrical source of radius,  $a = 1$  unit is considered the result obtained is compared with available theoretical solution. The pressure of pulsating cylinder, surface velocity  $u = U_0 \sin(\omega t)$ , at distance  $r$  from the center of the cylinder, can be deduce by [14]:

$$p(r, t) = i\rho c U_0 \frac{H_0^{(2)}(kr)}{H_1^{(2)}(ka)} e^{i\omega t} \quad (15)$$

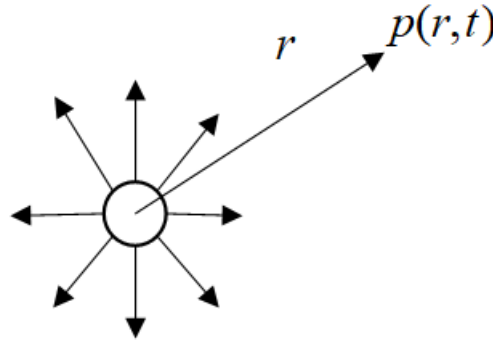


Figure 4. Schematic of cylindrical sound source and receiving point p at distance r from the source.

In Eq. (15),  $\rho$  is the density of medium,  $c$  is the speed of sound,  $U_0$  is amplitude of surface velocity of the cylinder.  $H_0^{(2)}$  &  $H_1^{(2)}$ , represent the *Hankel* function of second kind of order zero and first respectively. To validate the acoustic radiation from the numerical solver, first the spatial pressure distribution is computed using analytical formula from Eq. (15) and time history of the resultant pressure is recorded on circumference of radius,  $r=20$  units. The recorded pressure is then used as input in the numerical simulation considering as circular source of radius 20 unit, Figure 5 shows the schematic of implementation of analytical data as source in the numerical domain. The center position of the source is considered at the middle of a square computational domain of  $200 \times 200$  grid points with uniform grid

spacing of size 0.2 unit in both x and y directions. The results obtained from analytical and numerical approach are compared for two location at a radial distance  $r=40$  unit and  $r=60$  unit, as indicated by point  $P_1$  and  $P_2$  in Figure 5 respectively. Figure 6 shows the spatial distribution of pressure contours calculated by numerical solver.

Figure 7(a) and 7 (b) show time history of the measured sound pressure at the point  $P_1$  and  $P_2$  respectively. In Figure 7, the dotted line represents analytical pressure and solid line represents numerical pressure. The figure indicates that numerical results are in good agreement with analytical results at  $r = 40$  and  $r = 60$ .

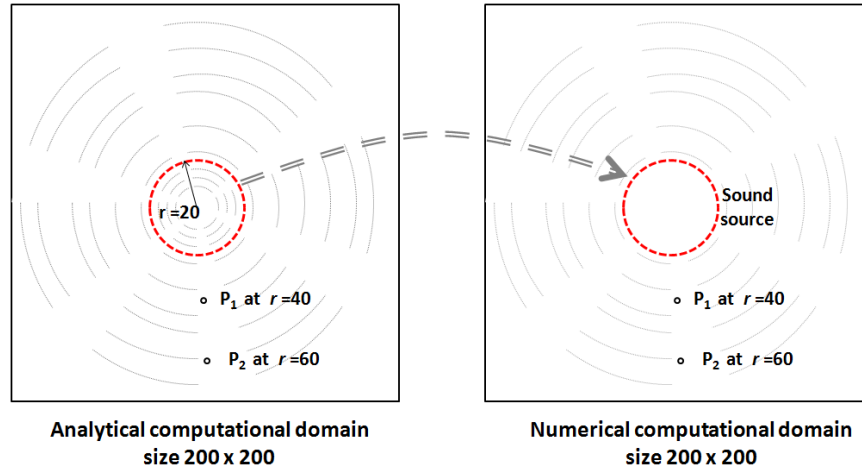


Figure 5: Schematic of consideration of source from analytical solution into numerical domain (figure not to scale)

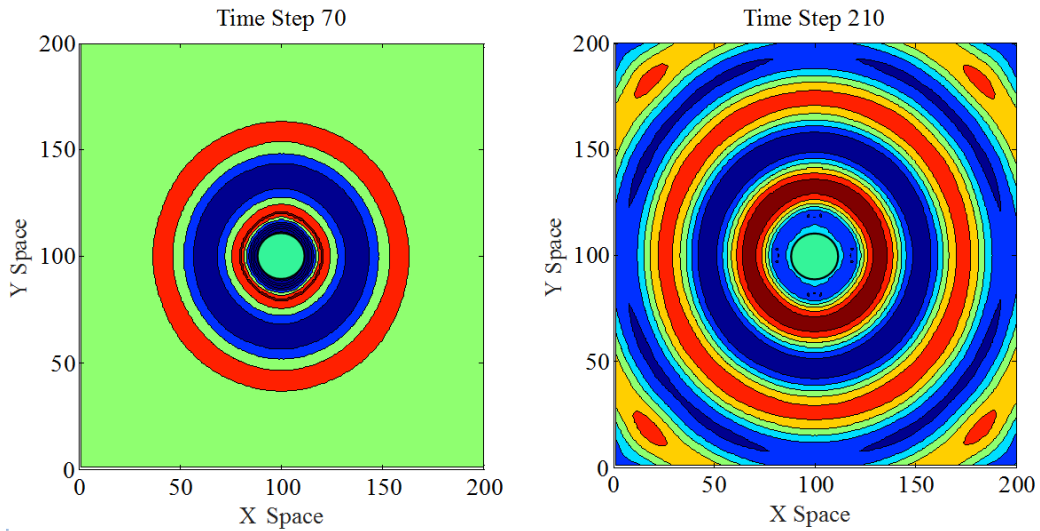


Figure 6: Spatial distribution of acoustic pressure calculated from numerical solver at time step 70 and 210.

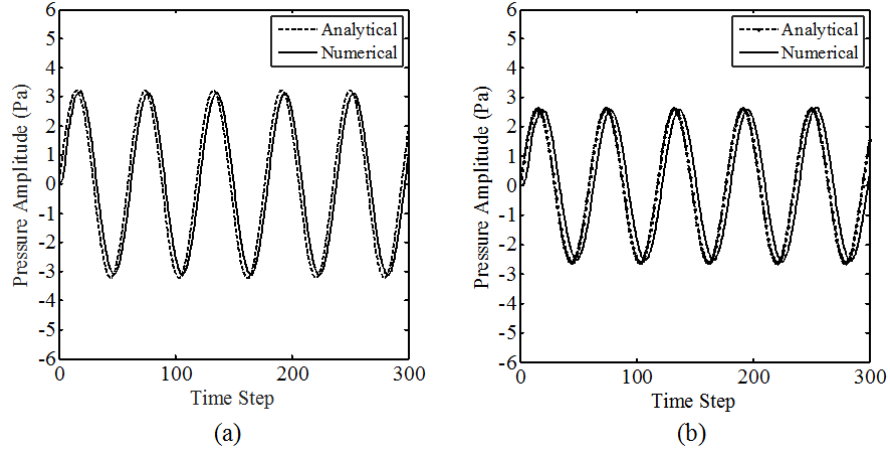


Figure 7: Time history of the measured sound pressure at radial distance 40 and 60 at points P<sub>1</sub> and P<sub>2</sub> as shown in Fig. 5.

Now, effect of various boundary conditions is analyzed for the case of two-dimensional wave propagation. A line source instead of point source, as considered in the previous study, is used. A rectangular duct of size  $200 \times 50$  grid points with uniform grid spacing of 0.2 in both x and y direction is considered. Except the right boundary wall, all other walls are fully absorbing. Figure 8 shows the line AB as the source of impulse sound and pressure field distribution at time step  $t=70$  and at  $t=145$ . The pressure pulse originated from line AB and propagated in both left (backward) and right (forward) directions. From the figure, it is observed that at instant  $t=70$ , both wave fronts are moving in opposite direction, however, at time step  $t=145$ , the right moving wave have already reflected from the wall and now moving towards the left boundary, however the left front still heading towards the left boundary. The light color contours behind the main wave front is presented due to numerical noise developed, which can be suppresses by adding proper numerical damping. However, in this simulation, the relative magnitude of the noise is very small and thus not ignored.

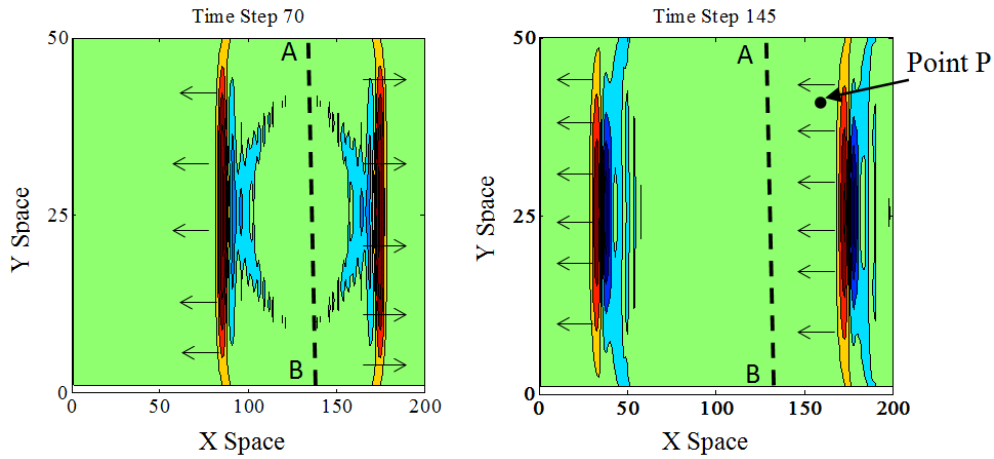


Figure 8: Spatial distribution of pressure with impulse source at time step of 70 & 145. The arrow indicates direction of motion of wave

Figure 9 shows the time history of incident and reflected (superimposed) sound wave at point P (indicated in Figure 8) for various reflection coefficient of the boundary. The figure is plotted for a harmonic line source of amplitude 5 Pa and frequency 100 Hz. The RMS pressure value observed at point P for different reflection condition is summarized in Table 2. From Table 2, column 2 and column 6, it can be noted that the amplitude of the reflected sound imitates the level of reflection ( $R$ ) considered in the wall surface.



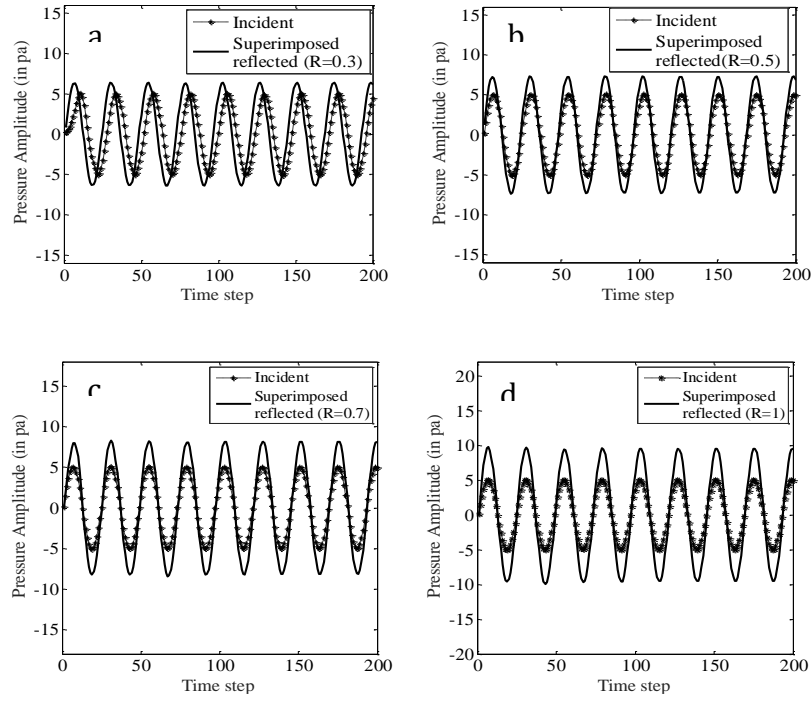


Figure 9. Comparison of incident and superimposed reflected wave in rectangular domain at point P using reflection coefficient of a) 0.3, b) 0.5, c) 0.7 & d) 1

Table 2: Comparison of RMS pressure amplitude corresponding to the various reflection coefficient of wall

Sr. No	Reflection Coefficient (R)	RMS Value of incident wave	RMS Value of superimposed-reflected wave	RMS value of reflected wave	Percentage change in RMS value
1	0.3	3.5049	4.5366	1.0317	29.43
2	0.5	3.5049	5.2094	1.7045	48.52
3	0.7	3.5049	5.8240	2.3191	66.17
5	1	3.5049	6.8260	3.3211	94.76

### 3. Sound propagation in a three dimensional space

In this section, a problem of sound propagation in a three dimensional room is carried out. It is worth to note that the computational domain, boundary conditions and sound source considered in this study are considered based on the enclosed space considered in the experimental study, Section 4. Figure 10 shows the schematic of the computational domain and placement of the source and receiver points. The numerical domain is discretized by considering a uniform grid size of  $\Delta x = \Delta y = \Delta z = 0.2$ . An optimal temporal step size  $\Delta t = 0.00022$  seconds is considered based on the CFL condition. The sound source is assumed at the center of the domain. The frequency of the sound radiating from the source is a combination of multiple frequencies of 116 Hz, 133 Hz and 216 Hz, which are considered based on the sound spectrum measured in the experimental study. The relative amplitude corresponding to the three frequencies are in same proportion as observed in the Fourier transformation of measured experimental data (Figure 13b).

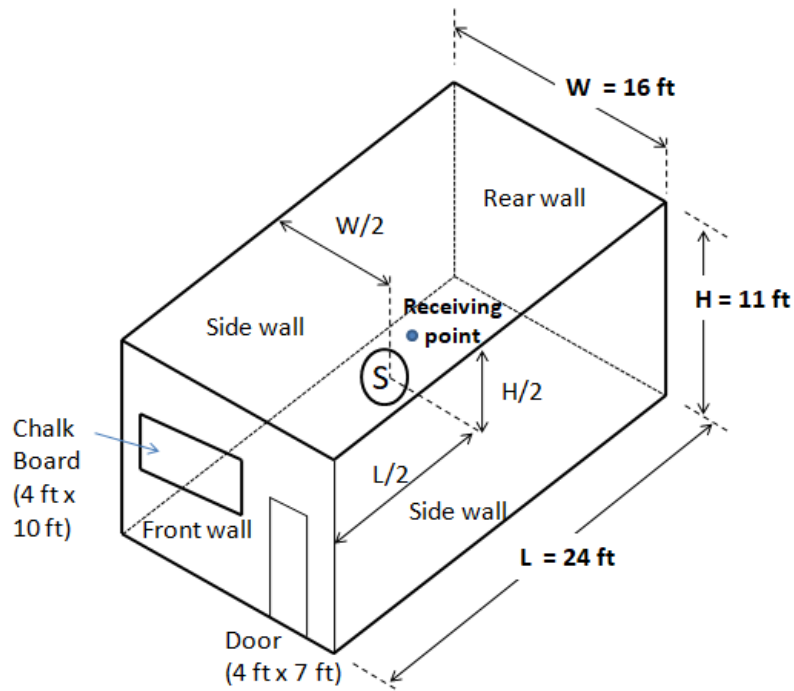


Figure 10: Schematic of computational domain (Figure not to scale)

Table 3 shows the reflection coefficient of various surfaces of the numerical domain that is equivalent to actual classroom [4-5].

Table 2. Reflection coefficient of material used at the wall of classroom

Faces	Reflection coefficients
Rear (glass)	0.9
Side faces (concrete)	0.8
Floor (concrete)	0.8
Ceiling (concrete)	0.8
Front face (combination of door, chalk board)	0.6

To simulate the reverberation effect in the room, first the periodic sound is allowed to propagate within the room for creating diffused sound field and then source is stopped to measure decay of sound. It may be noted that to get a diffused field, source must be kept on till the sound pressure level in the whole region becomes comparable. The diffused field can be checked by cross-measuring SPL at multiple locations. In the present simulation, due to limited computational resources, the sound is allowed to propagate for a limited time of 0.16 seconds, which may be extended to get more reliable diffused sound field. However, in this study, it is assumed that the in the considered time, diffused field generated after multiple reflection of the sound.

Figure 11 (a) indicates the time history of the SPL in dB of sound measured at receiving point (Figure 10). In the figure, point C shows the cut-off point, which indicates the instant when the sound source has been stopped. Figure 11 (b) shows the decay of sound obtained by exponential curve fitting approach on the data shown in Figure 11 (a). In the figure 11, the dots are pointing out the peak amplitude of the SPL and a continuous line indicates an exponential curve fitted using the peak points. It is observed that the sound pressure decays very fast in initially phase and reaches to steady state level. It may be noted that the sound level decays up to 69 dB (approximately) and remains steady further. It is expected that this level remains due to the numerical noise generated by the employed FDTD scheme. However, a decay of 20 dB is conveniently measured from the fitted curve and used to evaluate RT by extrapolating it for 60 dB drop ( $RT_{60}$ ) with linear assumption. A drop of sound pressure level from 89 dB to 69 dB indicates a reverberation time  $RT_{60}$  of 0.94 sec.

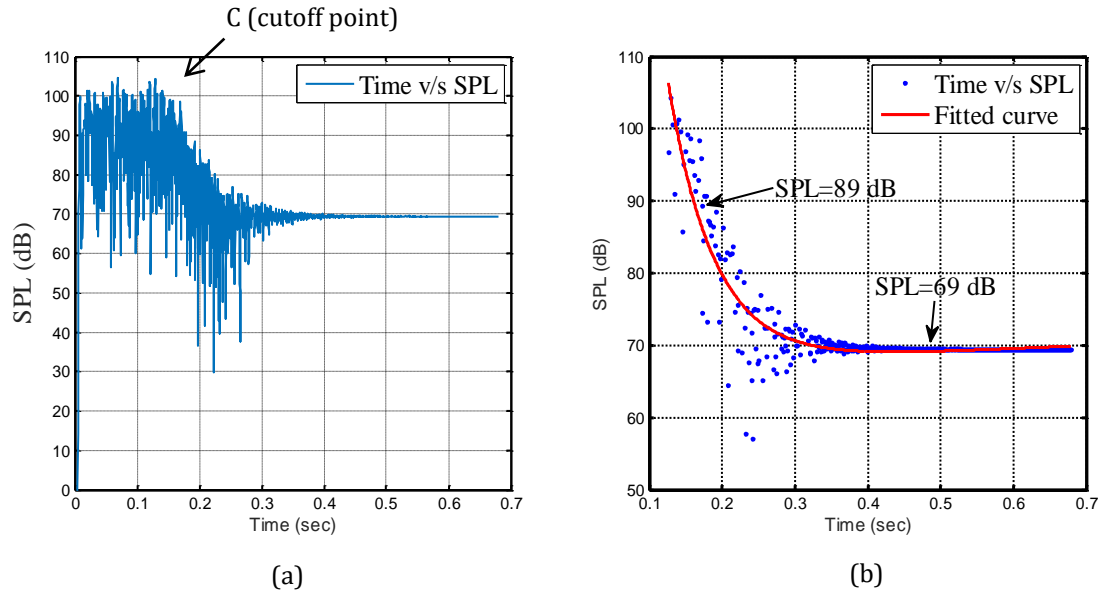


Figure 11. SPL decay of three dimensional computational domain

#### 4. Experimental Measurement

In this section, experimental measurement of reverberation time of a classroom of size  $24 \times 16 \times 11 \text{ ft}^3$  is discussed. The measurements are carried out using two approaches as by pricking a balloon and by a harmonic sound source (loudspeaker). The source is placed at the center of the room and the acoustic data is recorded using a microphone placed at 1 m away from the source. Figure 12 (a) and 12 (b) shows the actual picture of the classroom and a schematic indicating source and measurement location (figure not to scale). For the data acquisition, a  $\frac{1}{2}$  inch pressure microphone and an open source measurement tool “Audacity” is used. The data is measured at a sampling rate of 44100 Hz

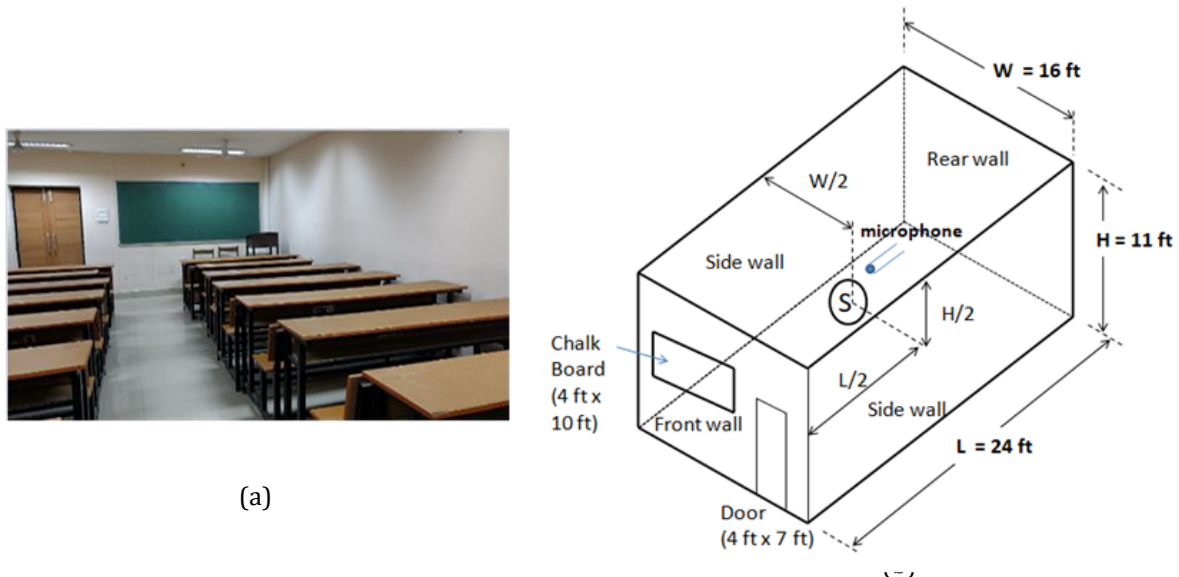


Figure 12: Actual picture of classroom and schematic of source and receiver location

In the first case, a balloon is burst and the sound pressure level is recorded. Figure 13 (a) shows the time history of the SPL measured, where in the solid line shows an exponential curve fitted using the measured data points. The experiments are performed a number of times and before taking final reading, repeatability of the measurement is also tested. Figure 13 (b) illustrates the frequency spectrum of the measured sound signal. The frequency spectrum indicates that the sound generated by the bursting has a dominating component corresponding to 216 Hz. It may be noted that to find the reasoning of presence of a

dominating peak, the tests are performed with different sizes of balloon, however, the dominating peak appeared in all the measurement. The reason of the dominating frequency component may be due to excitation of any of the room mode. In addition to that, a number of frequency components are presented in the spectrum. It is observed that the sound decay very fast and reaches to a steady state level of 60 dB (approximately). The steady state dB level may be considered as the background noise presented in the room. For the calculation of reverberation time ( $RT_{60}$ ), an attenuation of 20 dB (sound pressure level decay from 98 dB to 78 dB) is measured and extrapolated for a 60 dB drop assuming linear variation. In this case, the observed  $RT_{60}$  is 0.84 seconds.

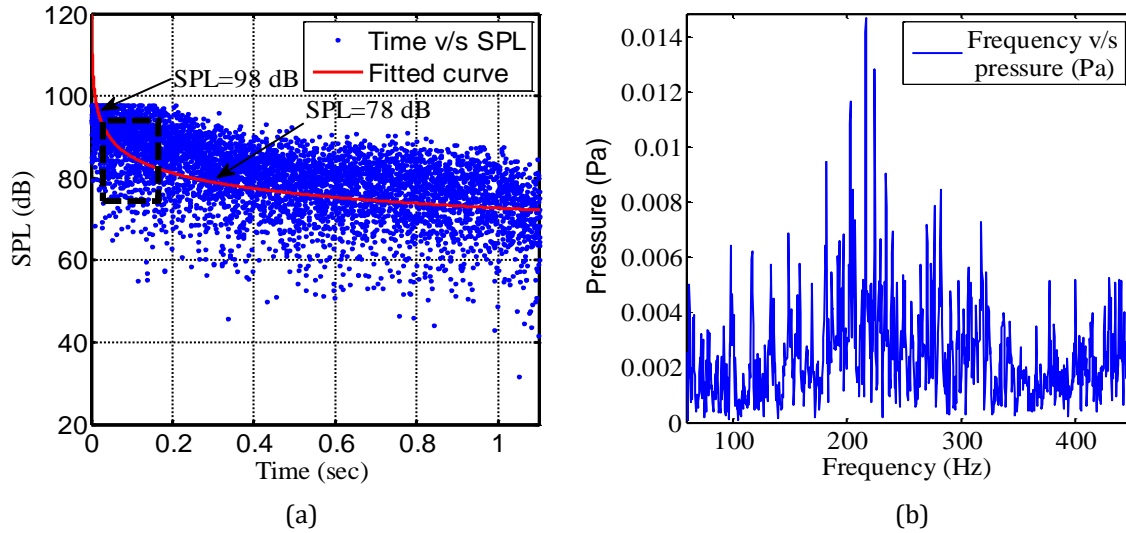


Figure 13. (a) Decay in sound pressure level of experimental data in case of balloon pricking (b) FFT of sound pressure data shown by a rectangular highlighted region in (a)

In the second case study, an un-baffled loudspeaker is used as sound source, which emits harmonic sound waves. The frequency of the emitting sound is selected based on the frequency generated by the normal speaking in the classroom. In the present investigation, combination of two different frequencies as 125, Hz, 280 Hz, which falls in the range of normal speaking are considered. Relative amplitude of both the frequency components is considered same. Before the measurement of reverberation time, the sound source is kept on for an adequate time (30 seconds), thus a diffused field can be created within the room. To ensure presence of diffused sound field within the room, SPL is measured at different location and after achieving a minimum difference of 1-2 dB the source is switched off and corresponding sound is recorded. Figure 14 (a) shows the time history of the SPL measured. In Figure 14 (b), the solid line shows an exponential curve fitted using the measured data points. From the figure, a 20 dB drop ranging from 89 dB to 69 dB is measured, which is extrapolated to give  $RT_{60}$  0.91 seconds.

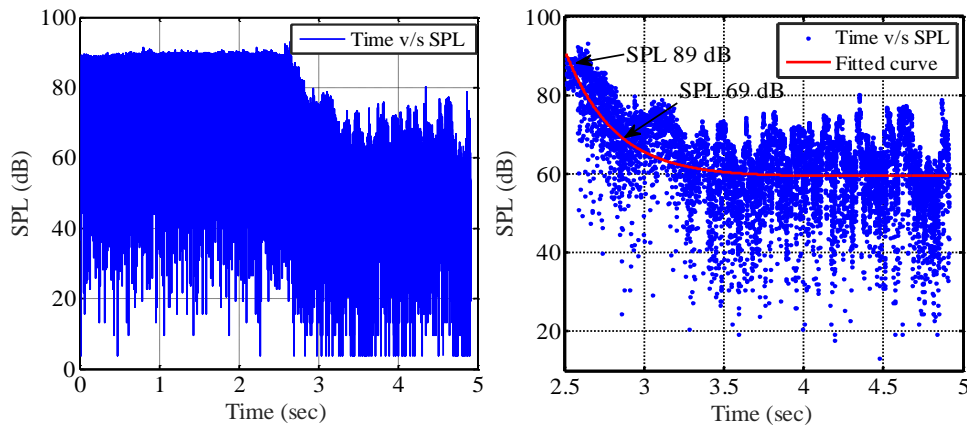


Figure 14. SPL decay of experimental data with an unbaffled loudspeaker

Table 4 shows the reverberation time measured by two different approaches. For the comparison, a reverberation time calculated from the analytical formula given by Sabine is also added. The Sabine's equation defined as

$$RT_{60} = \frac{0.16V}{\Sigma\alpha S} \text{sec} \quad (21)$$

where  $RT_{60}$  shows reverberation time,  $V$  is volume of enclosed space,  $\Sigma\alpha S$  effective absorbing area,  $\alpha$  is the average absorption coefficient of space and  $S = S_1 + S_2 + \dots + S_n$  is the total surface area of the room. In addition, the table also shows  $RT_{60}$ , obtained from the numerical study carried out for an equivalent three dimensional space.

Table 3. Comparison of experimental, analytical and numerical reverberation time in seconds

	BY balloon pricking	Using harmonic source	Using Sabine's equation	Numerical methodology
$RT_{60}$ of a room size $24 \times 16 \times 11 \text{ ft}^3$	0.84	0.91	1.1	0.94
% variation w.r.t. $RT$ measured for the case of harmonic source	8.3%	--	10.9%	3.2%

Table 4 shows that, in the experimental measurements (column 1 and 2), the reverberation time obtained by bursting a balloon is little lower than the case of a harmonic source. The difference may be due to the frequencies generated from the two different sources are different. In case of balloon, sound generated is of impulsive nature and contain wide range of frequencies, however, the loudspeaker emits harmonic sound. In case of experimental and analytical results (column 4, Table 4), a significant difference is noted between the experimental results and results obtained from the analytical approach (Sabine's equation). It may be due to that the analytical formulation involves a number of assumptions and primarily developed to give an approximation of the reverberation time of an enclosed space. It does not includes the effect of dissipation of sound within the room due to the medium as well as it does not take care of shape of the space where the wave is travelling, thus, a higher reverberation time is obtained from analytical formulation. In addition, in the actual classroom, installed furniture may absorb the sound that leads to a smaller reverberation time in the experimental measurement. The order of the reverberation time predicted by the numerical approach is found comparable with the experimental results. In the numerical method, the effect of the medium (dispersion, dissipation of sound) is considered, however in the modeling of the enclosed space, other objects as furniture etc. has been ignored. Nevertheless, the results are encouraging and, thus, the developed numerical formulation may be utilized to predict reverberation time of an enclosed space.

## 5. Conclusions

Investigation of sound propagation and its reflection, absorbtion from the wall boundary is an important aspect in architectural acousics. Even though, the propagation of sound waves has been reasearched from several decades, there are many fronts where numerical estimation of behaviour of sound in a closed space is a challenging task. In the presented work, a numerical solver has been developed to investigate the problem of room acoustics. The solver is developed using finite difference time domain (FDTD) technique with leapfrog scheme. Various boundary models are employed to illustrate reflection/absorbtion of sound from the boundaries. Investigations are carried out for one, two and three dimensional spaces. The developed methodology is also validated for different benchmark results. The effect of boundary is modeled by considering reflection coefficient of the wall surfaces. For a test model of a room, reverberation time is estimated by radiating the sound for a short periods and then by measuring the decay of sound at a point in the space. The attenuation of sound is plotted on dB scale and a drop of 20 dB is calculated, which is then extrapolated to estimate  $RT_{60}$ . Experiments are performed to measure the reverberation time of an classroom. Two different sound sources are tested for the calculation of  $RT_{60}$ . Measured data is analyzed by plotting time history and frequency spectrum of sound pressure level (SPL). The result obtained by experimentally measured reverberation time is compared with the numerical result and reasonable matching in the two data is noted. It is interpreted that the

difference between the two results may be due to the presence of furniture and other objects in the classroom, which have not been modelled in the numerical investigation.

From the aspect of accuracy of outcome of the work, bearing it in mind that the results obtained from the numerical tool is sensitive to input parameters e.g. modeling of absorption boundaries, modeling of acoustic domain and an improper inputs may lead to unreasonable result. In addition to this, suppression of numerical noise is another challenge and requires further development particularly in propagation of high frequency waves. In the current state, the numerical tool provides a reasonably good estimation of acoustics propagation in a closed room and corresponding RT. The results obtained help to have an initial gauge of acoustical characteristics of the room. However, to get very accurate RT, experiments can be performed. But, the experiments needed number of transducers and sophisticated tools to measure sound pressure distribution in room.

Nevertheless, the results are encouraging and suffice the application of the developed numerical tool to have a reasonable estimate the reverberation time of an enclosed room. From the measurement of the RT of classroom  $RT_{60}$  (0.94), which is not ideal for a classroom (ideal RT for classroom is 0.6-0.7 [1]), it may be inferred that there is a scope to make room more acoustically suitable.

## 6. References

- [1] Kuttruff, H. (2009) Room acoustics. : Spon Press, Abingdon, Oxon, UK.
- [2] Sabine, W.C. (1915), Architectural acoustics. Journal of the Franklin Institute. 179(1): p. 1-20.
- [3] Eyring, C.F. (1930), Reverberation time in "dead" rooms. The Journal of the Acoustical Society of America,. 1(2A): p. 217-241.
- [4] Delany, M. and E. Bazley (1970), Acoustical properties of fibrous absorbent materials. Applied acoustics, . 3(2): p. 105-116.
- [5] Wassilieff, C. (1996), Sound absorption of wood-based materials. Applied Acoustics. 48(4): p. 339-356.
- [6] Tang, P. and W. Sirignano (1973), Theory of a generalized Helmholtz resonator. Journal of Sound and Vibration. 26(2): p. 247-262.
- [7] Botteldooren, D. (1995), Finite-difference time-domain simulation of low-frequency room acoustic problems. The Journal of the Acoustical Society of America. 98(6): p. 3302-3308.
- [8] Kowalczyk, K. and M. van Walstijn (2008), Formulation of locally reacting surfaces in FDTD/K-DWM modelling of acoustic spaces. Acta Acustica united with Acustica. 94(6): p. 891-906.
- [9] Asakura, T., et al., Prediction of low-frequency structure-borne sound in concrete structures using the finite-difference time-domain method. The Journal of the Acoustical Society of America,. 136(3): p. 1085-1100.
- [10] Kowalczyk, K. and M. Van Walstijn, Wideband and isotropic room acoustics simulation using 2-D interpolated FDTD schemes. IEEE transactions on audio, speech, and language processing,. 18(1): p. 78-89.
- [11] Yamashita, O. (2015),, Reflective boundary condition with arbitrary boundary shape for compact-explicit finite-difference time-domain method. Japanese Journal of Applied Physics,. 54(7S1): p. 07HC02.
- [12] Bilbao, S. (2004), Wave and scattering methods for numerical simulation. : John Wiley & Sons.
- [13] Krüger, J. and M. Quickert (1997), Determination of acoustic absorber parameters in impedance tubes. Applied Acoustics, 1997. 50(1): p. 79-89.
- [14] Purohit, A., A.K. Darpe, and S. Singh (2014), A numerical investigation on effects of structural flexibility on aerodynamic far field sound. Computers & Fluids, 2014. 89: p. 143-152.

## List of Figures:

- Figure 1: Acoustic computational domain showing boundaries and corner point.
- Figure 2: One dimensional wave propagation and its reflection from boundary.
- Figure 3: Time history of incident and reflected wave (superimposed) at point P for reflection coefficient, a) 0.3, b) 0.5, c) 0.7 & d) 1.
- Figure 4: Schematic of cylindrical sound source and receiving point p at distance r from the source.
- Figure 5: Schematic of consideration of source from analytical solution into numerical domain (figure not to scale).
- Figure 6: Spatial distribution of acoustic pressure calculated from numerical solver at time step 70 and 210.

- Figure 7: Time history of the measured sound pressure at radial distance 40 and 60 at points P1 and P2 as shown in Fig. 5.
- Figure 8: Spatial distribution of pressure with impulse source at time step of 70 & 145. The arrow indicates direction of motion of wave .
- Figure 9: Comparison of incident and superimposed reflected wave in rectangular domain at point P using reflection coefficient of a) 0.3, b) 0.5, c) 0.7 & d) 1.
- Figure 10: Schematic of computational domain (Figure not to scale) .
- Figure 11: SPL decay of 3D computational domain.
- Figure 12: Actual picture of classroom and schematic of source and receiver location .
- Figure 13: (a) Decay in sound pressure level of experimental data in case of balloon pricking (b) FFT of sound pressure data shown by a rectangular highlighted region in (a).
- Figure 14: SPL decay of experimental data with an un baffled loudspeaker.

### List of Tables:

Table 1.Comparison of RMS values corresponds to reflection coefficient

Table 2: Comparison of RMS pressure amplitude corresponding to the various reflection coefficient of wall

Table 3.Reflection coefficient of material used at the wall of classroom

Table 4.Comparison of experimental, analytical and numerical reverberation time in seconds